Supplemental information 1

As shown in **Fig. S1**, the local Gd concentration values varied between 0 and 1.1 wt.% when calibration curve-A cases were implemented. According to **Fig. S1**, R-4 was distinguishable and estimated as a region with a higher Gd concentration, whereas R-2 and R-5 could not be distinguished from the background. Therefore, to show the dominant concentration values in these quantitative maps, frequency histograms with a bin width of 0.04 wt.% (the lowest LOD value estimated from the calibration curve) were plotted in two regions (hereinafter referred to as region-1 and region-2). Region-1 holds the intensity values from measurement positions 1–400 where R-4 existed, whereas region-2 has the intensity values from measurement positions 401–800 where R-2 and R-5 existed. In these frequency histograms, the horizontal axis represents the Gd concentration, whereas the vertical axis represents the number of values in a certain bin. The reference concentration values are shown in red in the histograms, whereas the estimated LOD values from calibration curve-A are drawn using dotted black lines in each histogram. When calibration curve-A drawn by Gd (I) 501 nm was implemented, in region-1, two peaks at 0.04 wt.% and 0.84 wt.% were observed, whereas, in region-2, a peak at 0.04 wt.% was observed. The peak at 0.84 wt.% corresponds to R-4 of sample-1. According to the histogram plotted for region-1, the concentration values at the Zr metal (no Gd) regions were estimated to be between 0 and 0.24 wt.%, which is the same for region-2. Therefore, R-2 could not be distinguished because its true concentration value was 0.09 wt.%.

In contrast, when calibration curve-A drawn by Gd (I) 510 nm was implemented, in region-1, two peaks at 0.04 wt.% and 0.92 wt.% were also observed. The peak at 0.92 wt.% corresponds to R-4 of sample-1. In this case, the concentration values in Zr metal (no Gd) regions were also estimated to be between 0 and 0.24 wt.%. Unlike the case for Gd (I) 501 nm, in region-2, two peaks at 0.04 and 0.34 wt.% were observed. Because the concentration values were estimated to be in the range of 0.24–0.4, R-2 of sample-1 was visible in the quantitative map drawn by Gd (I) 510 nm. However, it shows a large deviation from the true concentration value.

As shown in **Fig. S2**, the estimated Gd concentration values varied from 0 wt.% to 1.5 wt.% when calibration curve-B was implemented in the measurement dataset. When the calibration curve-B method was implemented on the dataset, measurement positions where Gd and Ce emission intensity values were more than 5×10^4 were only considered for calculation. Therefore, R-5 was filtered out from the dataset. To show the dominant concentration values, frequency histograms with a bin width of 0.04 wt.% were plotted for each case, and the histograms are shown in **Fig. S2(b)**. Unlike calibration curve-A, the measurement dataset was not divided into two regions because the estimated Gd concentration values for R-2 of sample-1 were lower than the LOD values (**see Fig. S2(b)**). Therefore, R-2 of sample-1 could not be quantified using calibration curve-B. In contrast, when calibration curve-B was implemented, the concentration values for R-4 of sample-1 were estimated to be slightly larger than the true value in all four cases. The ratio between Gd 501 nm and Ce 527 nm shows the best result, which is close to the true Gd concentration.

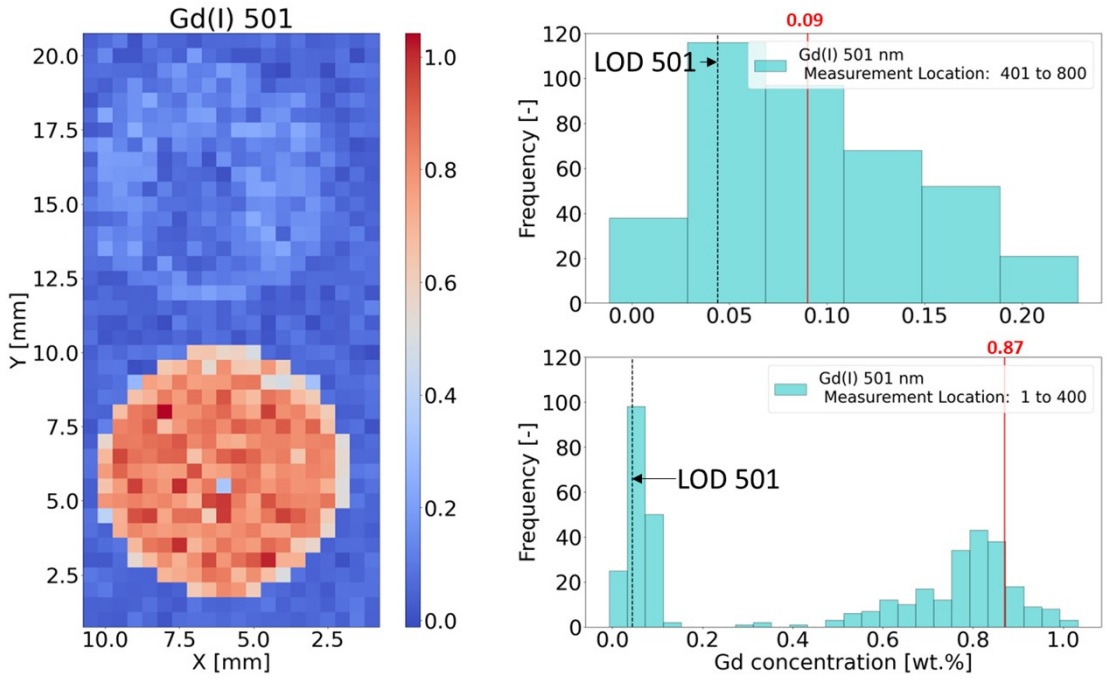

(a)

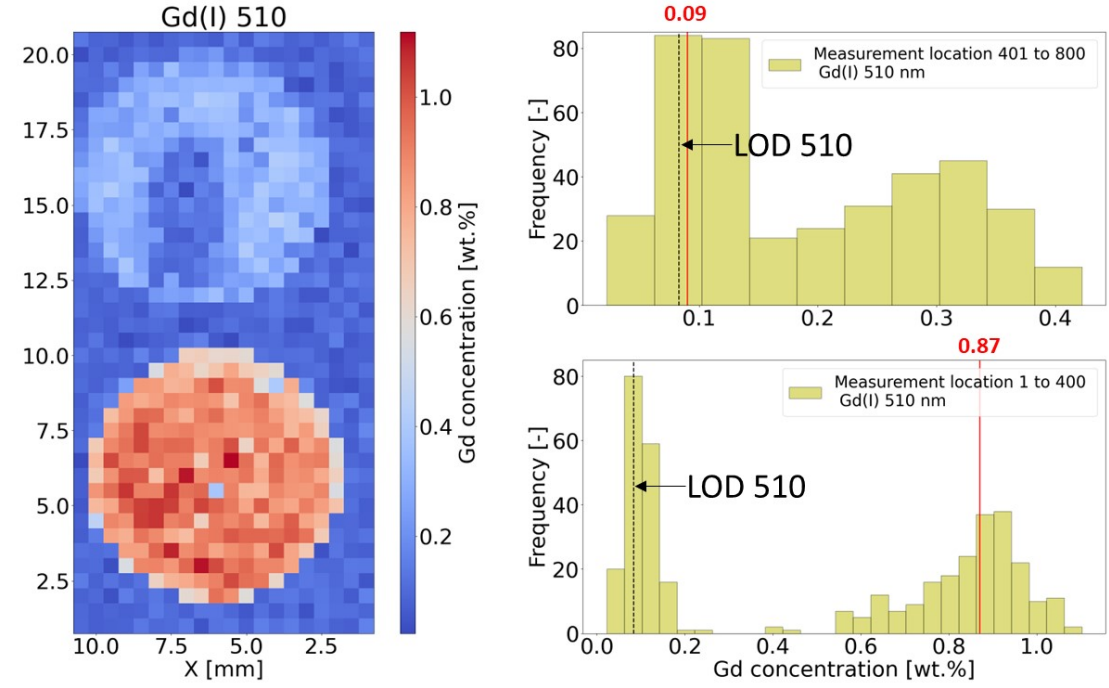

(b)

Fig. S1. Quantitative Gd map using the calibration curve-A method.

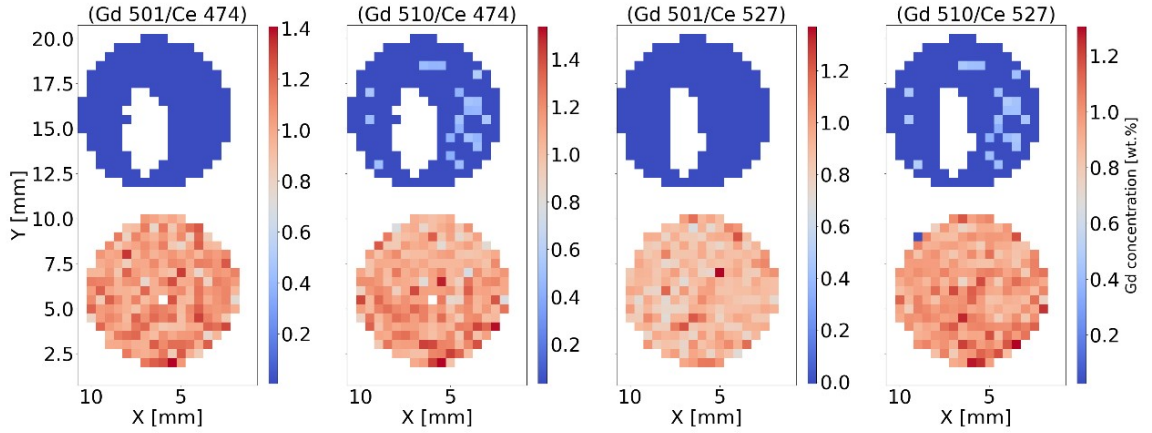

(a)

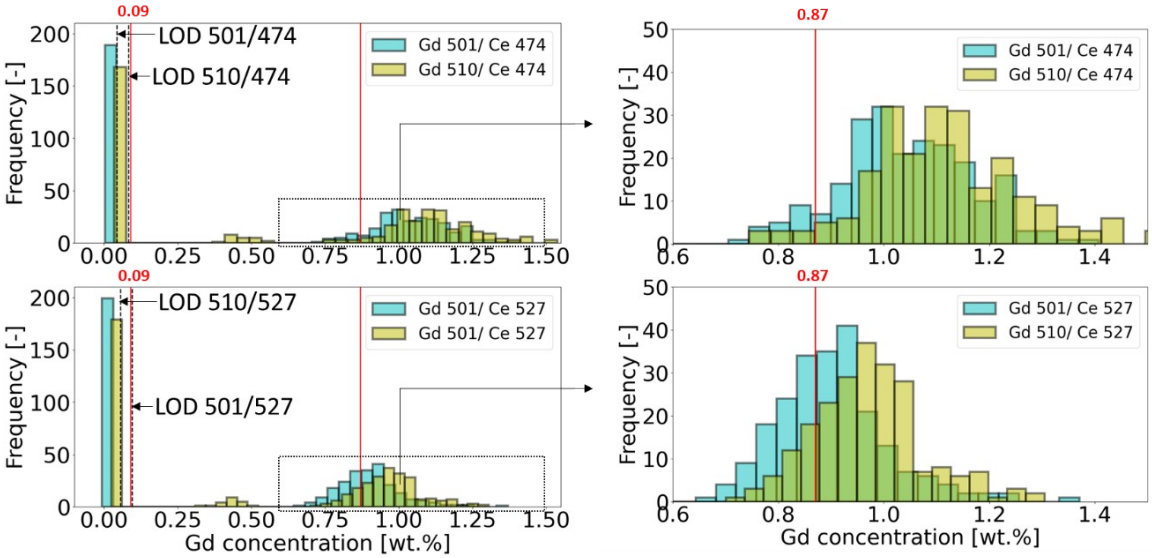

(b)

Fig. S2. Quantitative Gd map using the calibration curve-B method.

Supplemental information 2

An image reconstructed using peak-to-peak amplitude is shown in **Fig. S3**. The peak-to-peak value estimated in R-5 was weak because R-5 existed in the defocusing range of the incident laser where weak plasma was generated.

Furthermore, as shown in **Fig. S3**, because of the sample height and a-distance (laser head and microphone arrangement), the peak-to-peak amplitudes of the recorded wave differed between the two sides of the sample. At the right-hand side of the sample where weak signals are detected, only a part of the acoustic energy might be detected by the microphone because part of the acoustic waves can be blocked by the sample height. At the left-hand side of the image, the acoustic energy detected without any blockage and the reflected acoustic waves might enhance the amplitude of the waveform. Therefore, a coaxial configuration of a laser and microphone or an additional microphone should be preferred for the future design of AW-mLIBS.

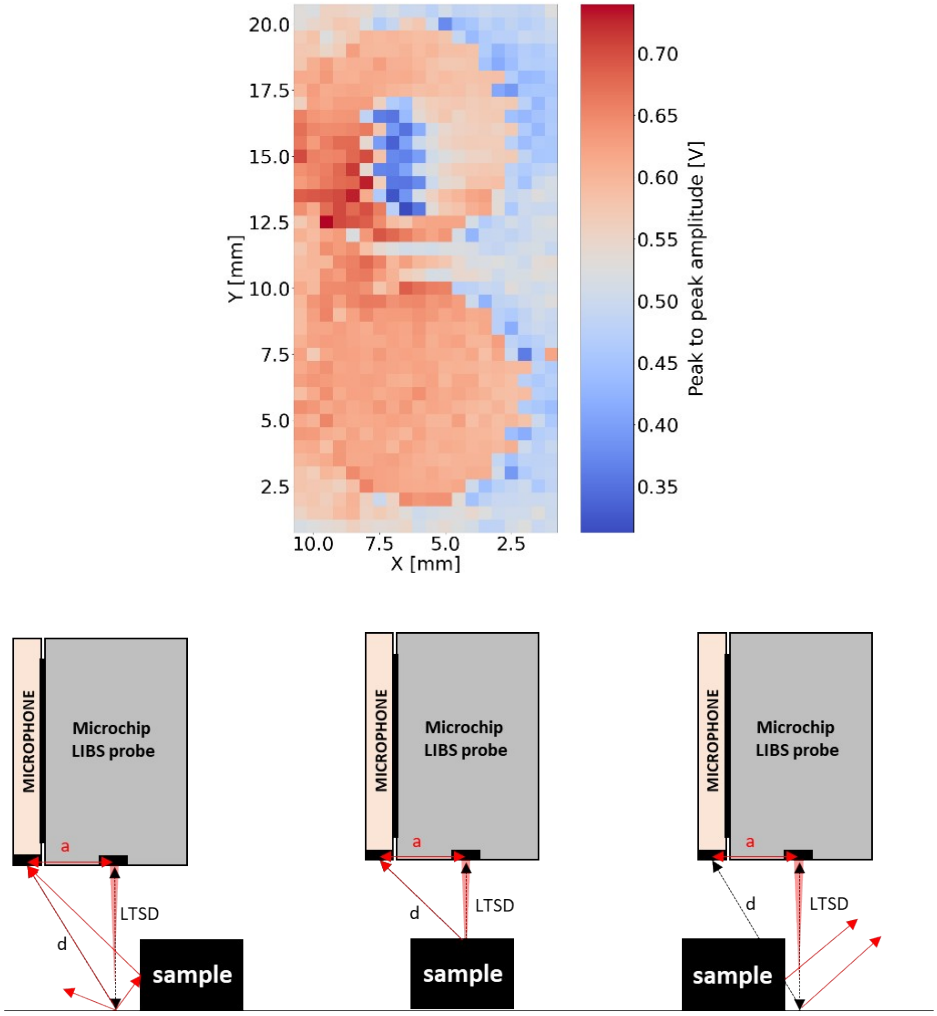

Fig. S3. The peak-to-peak amplitude and the effect of a-distance.